A Solution of the X-ray 'Phase Problem'*

By BEN POST†

Physics Department, Polytechnic Institute of New York, 333 Jay Street, Brooklyn, New York 11201, USA

Abstract

The phases of X-ray reflections are lost in the diffraction process in conventional two-beam diffraction. It is shown that the phases are not lost when three beams diffract simultaneously, and that phase information can be extracted from knowledge of the spatial distribution of the diffracted intensities about the three-beam point. In centrosymmetric crystals, the distribution is a sensitive function of the invariant phase of the product of the structure factors involved in simultaneous diffraction. High-resolution divergent-beam photographs illustrating the intensity differences associated with positive and negative triplet-phase products are shown.

Introduction

It has long been suspected that coherent interactions among diffracted X-ray beams which take place when several sets of planes diffract simultaneously may provide clues to a solution of the X-ray 'phase problem'. For this reason, simultaneous n-beam diffraction ($n > 2$) has been investigated by Lipscomb (1949), Eckstein (1949), Fankuchen (1949), Miyake & Kambe (1954), Kambe (1957), Hart & Lang (1961), and many others, but with only limited success.

In general, the phases of the structure factors of individual reflections from single crystals vary with the position assigned to the origin of the unit cell. Such phases are clearly unsuited for experimental determination. The products of the phases of groups of structure factors whose diffraction vectors form closed polygons are, however, invariant to choice of origin, and *their* determination does have physical significance. In this work we will be concerned with the experimental determination of such invariant quantities in centrosymmetric crystals whose origins are at centers of symmetry. Groups of structure factors of centrosymmetric crystals involved in simultaneous n-beam diffraction satisfy these requirements.

A procedure for generating three-beam diffraction systematically is illustrated in Fig. 1. When reciprocal-lattice point (rlp) H is brought to its diffracting position on the surface of the Ewald sphere, two-beam diffraction occurs. Diffracted beams are directed to O and H. If the crystal is rotated about $\overrightarrow{OH}$, additional rlp's (*e.g.* P) are brought successively to their diffracting positions. In each such instance simultaneous n-beam diffraction will occur so long as the setting of H on the Ewald sphere remains undisturbed.

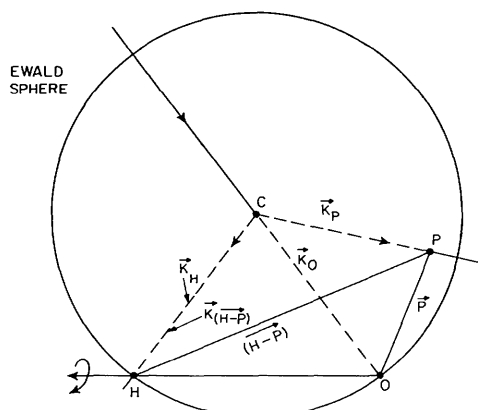An alternative representation of three-beam diffraction, within the crystal, is given in Fig. 2. The incident
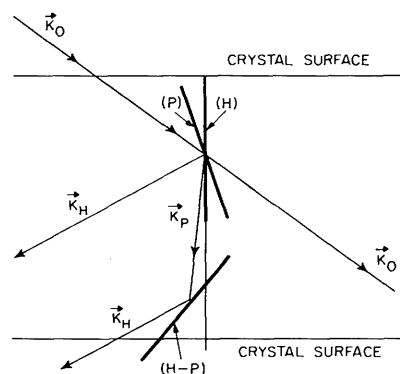

Fig. 1. Simultaneous n-beam diffraction.

Fig. 2. Transmission of simultaneous three-beam diffraction through a crystal.

beam satisfies Bragg's law for diffraction by planes (H) and (P). The Bragg conditions may be written as:

$$\mathbf{K}_H - \mathbf{K}_O = \mathbf{H}, \tag{1}$$

$$\mathbf{K}_P - \mathbf{K}_O = \mathbf{P}. \tag{2}$$

The K's are the propagation vectors of the incident and diffracted beams. The rlp's to which they are directed are indicated by the subscripts. Subtraction of equation (2) from (1) gives:

$$\mathbf{K}_H - \mathbf{K}_P = (\overrightarrow{H - P}) \tag{3}$$

in which $\mathbf{K}_P$ serves as the 'incident' beam vector. It is diffracted by the ($H - P$) planes in the $\mathbf{K}_H$ direction. Under such conditions, parallel, overlapping, coherent beams are simultaneously directed to all the rlp's in diffracting positions. It is evident that simultaneous n-beam diffraction can provide the necessary conditions for interference among discrete coherent beams, in simple, controllable form.

Theory

The kinematical theory of X-ray diffraction is used extensively in crystal structure analysis, but it is unsuited for the detailed analysis of wave fields in crystals, which is needed for phase determination. For the latter purpose, Ewald's (1916, 1917) self-consistent n-beam dynamical theory of diffraction provides an ideal tool. Excellent reviews of the basic theory are available: Batterman & Cole (1964); James (1963); Schwartz & Cohen (1977).

The X-ray wavefields in n-beam diffraction obey Maxwell's equations for a medium with a complex, periodic dielectric constant. A sum of plane waves satisfying Bragg's Law is taken as the assumed solution for the wavefield:

$$\mathbf{D} = \sum_H \mathbf{D}_H \exp\{-[2\pi i(\mathbf{K}_H \cdot \mathbf{r} - vt)]\}. \tag{4}$$

Using Bragg's Law ($\mathbf{K}_H = \mathbf{K}_O + \mathbf{H}$) we have

$$\mathbf{D} = \exp\{-[2\pi i(\mathbf{K}_O \cdot \mathbf{r} - vt)]\} \sum_H \mathbf{D}_H \exp(-2\pi i \mathbf{H} \cdot \mathbf{r}). \tag{5}$$

$\mathbf{K}_H$ is the wave vector within the crystal, directed to rlp H; $\mathbf{D}_H$ is the displacement vector, transverse to $\mathbf{K}_H$.

The solutions of Maxwell's equations lead to a set of linear homogeneous equations for the amplitudes:

$$2\varepsilon_H \mathbf{D}_H = -\Gamma \sum_P F_{(H-P)} \mathbf{D}_{P_{[H]}}, \tag{6}$$

an expression first derived by Ewald (1917). $F_{(H-P)}$ is a structure factor; $\mathbf{D}_{P_{[H]}}$ is the vector component of $\mathbf{D}_P$ which is perpendicular to $\mathbf{K}_H$. ε_H is a negative quantity defined by $|\mathbf{K}_H| = |k|(1 + \varepsilon_H)$; k is the vacuum wave vector; Γ is a constant equal to $e^2 \lambda^2/4\pi^2 \varepsilon_o mc^2 V$; V is

the volume of the unit cell and the other terms have their usual meanings. The summation is over all rlp's, but it is limited in practice to terms for which the ε's are very small. The corresponding rlp's are then in position to diffract. The permitted values of ε_H are the solutions of the secular determinant of equation (6). At the exact n-beam setting all the ε's are equal.

Equation (6) yields 'n' vector equations for n-beam diffraction. To deal with polarization, it is convenient to decompose each $\mathbf{D}_H$ into two mutually perpendicular components: D_H^σ and D_H^π. $2n$ scalar equations must then be taken into account. Usually, the solutions are obtained in the form of closely spaced pairs. The relatively minor differences between members of each pair are due to polarization effects. To minimize geometrical complexity, we will ignore polarization in our discussion. No significant loss of generality results, and the number of equations is cut in half. In our *calculations*, however, all $2n$ equations are taken into account.

In two-beam diffraction only two rlp's are in their diffracting positions. The corresponding solutions of equation (6) are readily obtained:

$$F_H^2 = \pm \left(F_o + \frac{2\varepsilon_o}{\Gamma}\right)^2. \tag{7}$$

The magnitudes of the solutions are independent of the phases of the structure factors. It can be concluded, therefore, that in two-beam diffraction it is not possible to determine the phases directly from the diffracted intensities.

The determinant of the coefficients of the D's, in the three-beam version of equation (6), is given in equation (8). The latter is set equal to zero to avoid trivial solutions.

$$\begin{vmatrix} \left(F_o + \dfrac{2\varepsilon_o}{\Gamma}\right) & F_{(-H)} & F_{(-P)} \\[2mm] F_{(H)} & \left(F_o + \dfrac{2\varepsilon_o}{\Gamma}\right) & F_{(H-P)} \\[2mm] F_{(P)} & F_{(P-H)} & \left(F_o + \dfrac{2\varepsilon_o}{\Gamma}\right) \end{vmatrix} = 0. \tag{8}$$

Expansion of the determinant yields a cubic equation:

$$\left(F_o + \frac{2\varepsilon_o}{\Gamma}\right)^3 - \left(\sum_3 F_i^2\right)\left(F_o + \frac{2\varepsilon_o}{\Gamma}\right)$$
$$+ 2F_H F_P F_{(P-H)} = 0. \tag{9}$$

Examination of equation (9) reveals that the permitted values of ε_o are strongly phase dependent. The equation has three unequal real roots, summing to zero. The distribution of the signs of the roots is determined

by the sign of the last term, *i.e. by the sign of the invariant phase of the structure factor triplet.* If one of the F's equals zero, the structure factor product vanishes; one root then equals zero and the other two equal $\pm$ the geometric mean of the non-zero structure factors. In the general case the two possible distributions of the roots, $(-++)$ or $(+--)$, lead to propagating modes which can differ significantly with respect to excitation and absorption.

Calculations

The general solution for the ε's near an n-beam point is usually represented by surfaces ('sheets') in reciprocal space. These define the possible origins of the wave-vector sets: $\mathbf{K}_O$, $\mathbf{K}_H$, $\mathbf{K}_P$. The collection of sheets for all the modes is the 'dispersion surface'. A calculated section through a dispersion surface is shown in Fig. 3.* The plane of the section is the perpendicular bisector of OH. The pairs of approximately horizontal curves in the right- and left-hand portions of Fig. 3 are the loci of points ('tie-points') at which the diffraction conditions for two-beam (O, H) diffraction are satisfied. Movement along these curves, for example from left to right, corresponds to rotation of the crystal in the opposite sense. Near the center of the figure, at $\Delta\varphi = 0$, the conditions for simultaneous diffraction involving rlp P are also satisfied. The exact, geometrical three-beam setting lies along $\Delta\varphi = 0$. Transitions from two- to three-beam diffraction take place between the three-beam setting and the two-beam regions. The distortion of the two-beam dispersion surface by the three-beam interaction is shown clearly in the figure.

---

* Figs. 3 and 4 have been calculated for both positive and negative triplet-phase products. The 'negative' calculations are shown when the figures are rotated by 180° from their 'normal' positions.
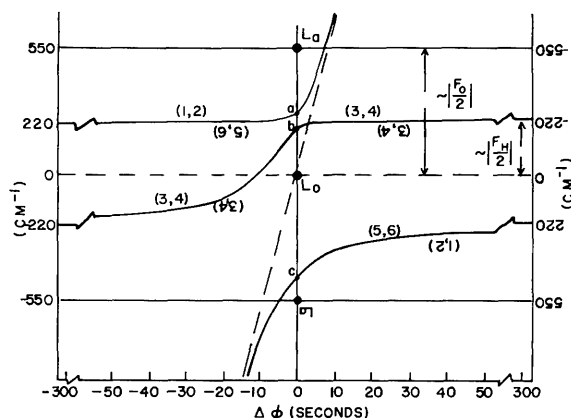

Fig. 3. Calculated section through a dispersion surface.

Because polarization effects are not included in Fig. 3, only two modes of propagation are shown in each two-beam region. These are labelled (1,2) and (3,4) to the left, and (3,4) and (5,6) to the right. The two digits within each set of parentheses designate the two modes that are normally operative and that would be shown if polarization effects were taken into account in the figure.

'La' and 'Lo', along $\Delta\varphi = 0$, are the three-beam Laue and Lorentz points. The horizontal lines passing through these points are referred to as the Laue and Lorentz lines. They are at reciprocal distances of $1/\lambda$ (vacuum) and $1/\langle\lambda \text{ (crystal)}\rangle$ from each of the active rlp's: O and H in two-beam regions, and O, H and P at the exact three-beam setting. The separation of these lines is proportional to $1 - \langle n_{\text{(crystal)}}\rangle$ and to the average electron density in the crystal (Batterman & Cole, 1964). Fig. 3 was calculated for F_o equal to 150 electrons, and for F_H, F_P, and $F_{(H-P)}$ equal to 50, 55 and 60 electrons respectively. The locations corresponding to the three-beam roots are indicated by a, b and c. In Figs 3, 4 and 5, $\Delta\varphi$ represents the angular deviation from exact three-beam setting.

The signs of the roots of equation (9) are $(-++)$ for a positive triplet phase and $(+--)$ for a negative phase. The roots have large values if the triplet includes strong reflections. If a negative phase is assumed for the triplet, the largest root must be positive. In some cases its magnitude may exceed F_o; if it does, the negative phase must be discarded. No comparable restriction applies to the roots for positive phases. The behavior of certain 'inequalities' used in crystal structure analysis is very similar to the above.

In general, the modes whose sheets are closest to the Laue line have the lowest absorption coefficients and are responsible for most of the transmitted intensities (Ewald & Héno, 1968). For positive phase these are the (1,2) modes on the left and (3,4) on the right. The corresponding modes are easily identified on the rotated (negative) plot. For a positive triplet phase, the curves corresponding to these modes are approximately symmetrical about the three-beam region. For negative phase, however, the curves show a large gap to one side of the three-beam setting, and the (3,4) curve on the right reaches positions equivalent to those of (1,2) on the left only at relatively large $\Delta\varphi$. These left–right differences lead to differences between the spatial distributions of the diffracted intensities for positive and negative phases. The positive–negative differences are maximized when all three F's are equal.

The intensity of beam H is proportional to $|\mathbf{D}_H|^2$:

$$I_H =$$

$$\left(\sum_m \{\mathbf{D}_H(m)\exp[2\pi i\mathbf{K}'_H(m).\mathbf{r}]\}\{\exp[-2\pi\mathbf{K}''_{(m)}.\mathbf{r}]\}\right)^2,$$

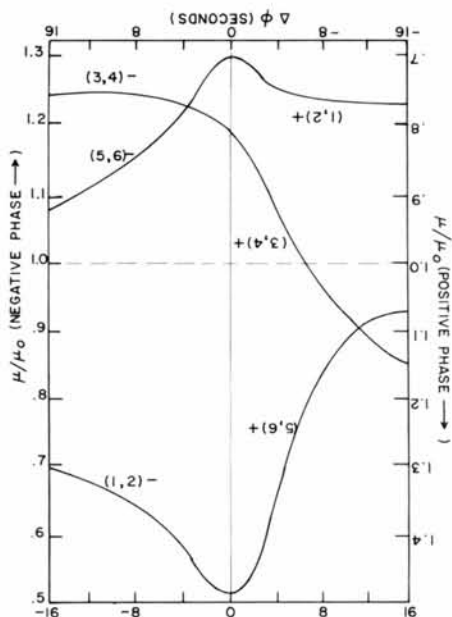where $\mathbf{K}_H = \mathbf{K}'_H - i\mathbf{K}''_H$. The sum is over the modes of

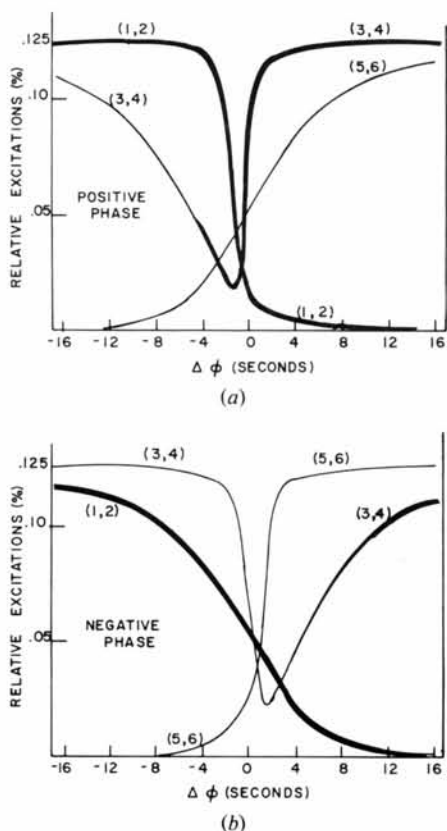Fig. 4. Relative absorption coefficients in three-beam diffraction, calculated for positive and negative phases.

propagation, m. The excitations of modes of propagation and the absorption coefficients are determined by the terms in the first and second sets of curly brackets respectively.

Fig. 4 shows the relative absorption coefficients of the modes, μ_m/μ_o. We note that the left–right differences among curves, representing the low absorption modes, are small for positive and much larger for negative phase.

Plots of excitations are shown in Fig. 5(a) and (b). The curves have been thickened to show where μ_m/μ_o is less than unity. The weighted excitation curves show the same types of phase dependence of the spatial distributions on the diffracted intensities as did Figs. 3 and 4.

Experimental

The phase effects discussed in the preceding sections have been investigated experimentally using essentially perfect germanium crystals about 0·4 mm thick, and

(a)

(b)

Fig. 5. Excitations of modes of propagation, calculated for (a) positive and (b) negative phases. Heavy lines show regions where μ/μ_o is less than unity.

HKL	F_c
112	−47
120	+60
012	−47

(a)

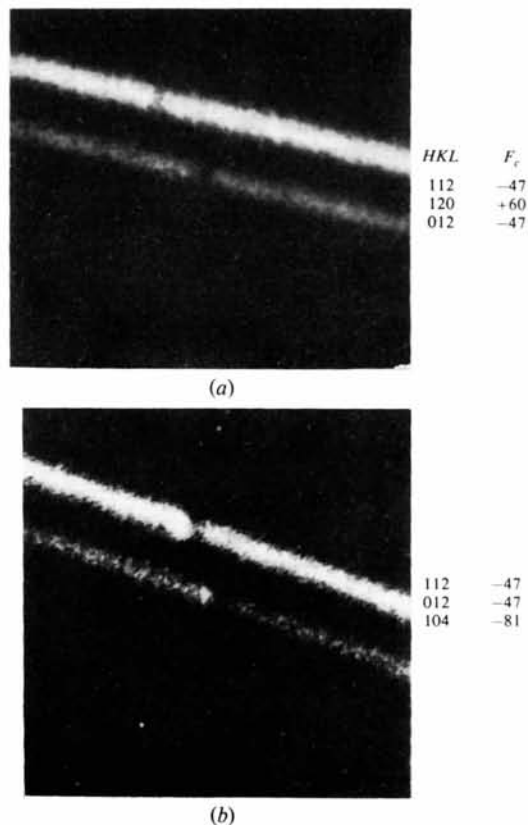|	
112	−47
012	−47
104	−81

(b)

Fig. 6. Divergent-beam photographs of three-beam diffraction in α-aluminum oxide. (a) Positive triplet phase. (b) Negative triplet phase.

relatively imperfect crystals of α-aluminum oxide, about 0·2 mm thick. The phases of the reflections are, of course, well known for both materials.

To achieve adequate resolution, a microfocus divergent X-ray beam was used. The X-ray source was a Cu K target; the focus was about 40 μm in diameter. At the take-off angles used in this work (4 to 8°), the effective focal spot was about 40 × 5 μm. The specimen crystals were oriented so that the smaller dimension determined the resolution along the two-beam reflection lines shown in Fig. 6(a) and (b). The source-to-crystal distance was 80 mm; the specimen-to-film distance was 1650 mm. The latter path was evacuated.

About 25 three-beam interactions in germanium and aluminum have been recorded photographically, using Kodak Type A film.* Fig. 6(a) and (b) illustrates the results obtained and shows two-beam Cu $K\alpha_1$ and α_2 ($1\bar{1}2$) reflection lines. The three-beam interaction regions are near the centers of the photographs. In Fig. 6(a) (positive phase) there is no significant difference between the intensities recorded to the left and right of the three-beam region. The left–right intensity differences calculated for negative phases are clearly displayed in Fig. 6(b). In fewer than half of the photographs were the positive–negative intensity differences too small to permit definitive phase assignments. Most of these difficulties appeared to be caused by our selection of relatively unfavorable triplets for study, i.e. cases in which the magnitudes of the three F's differed widely from one another. None of the photographs, however, indicated phases at variance with the known, correct ones.

---

* The photographs were taken by Mr Po Wen Wang, to whom the author is deeply grateful.

Summary

The phases of X-ray reflections from single crystals are not lost when three-beam simultaneous diffraction occurs. They may be determined by analyzing the distribution of the diffracted intensities about the three-beam point, under the conditions outlined in the preceding sections. It is not yet possible to indicate the extent to which the phase-determining methods described above can be applied to the 'mosaic' crystals usually used in crystal structure analysis. Our experience with relatively imperfect aluminum oxide crystals shows that the crystals need not be ideally perfect. Additional work with highly imperfect crystals is needed. The strictly collimated and highly intense X-ray beams available from synchrotron sources appear to be ideally suited for investigations of this sort.

References

BATTERMAN, B. W. & COLE, H. (1964). Rev. Mod. Phys. 36, 681–717.
ECKSTEIN, H. (1949). Private communication to Lipscomb (1949).
EWALD, P. P. (1916). Ann. Phys. (Leipzig), 49, 1–38.
EWALD, P. P. (1917). Ann. Phys. (Leipzig), 54, 519–597.
EWALD, P. P. & HÉNO, Y. (1968). Acta Cryst. A24, 1–15.
FANKUCHEN, I. (1949). Private communication; also quoted by Lipscomb (1949).
HART, M. & LANG, A. P. (1961). Phys. Rev. Lett. 7, 120–122.
JAMES, R. W. (1963). Solid State Phys. 15, 53–220.
KAMBE, K. (1957). J. Phys. Soc. Jpn, 12, 13–31.
LIPSCOMB, W. N. (1949). Acta Cryst. 2, 193–194.
MIYAKE, S. & KAMBE, K. (1954). Acta Cryst. 7, 218–220.
SCHWARTZ, L. H. & COHEN, J. B. (1977). Diffraction from Materials, ch. 8. New York: Academic Press.

Computer-Simulation Methods in X-ray Topography*

BY J. R. PATEL

Bell Laboratories, Murray Hill, NJ 07974, USA

Abstract

Complex diffraction contrast features on X-ray topographs are often difficult to interpret by simple arguments. In such cases computer-simulation methods have frequently proved useful in understanding the observed contrast features and in elucidating the nature of the defect involved. The application of computer-simulation methods for interpreting X-ray diffraction contrast at planar and line defects in crystals is outlined.

---

* This paper was presented, by invitation, at the ACA Dynamical Diffraction Symposium held at the University of Oklahoma, 22 March 1978, honoring Paul P. Ewald on the occasion of his ninetieth birthday.

There are many instances in X-ray topography where detailed analyses of the various complex contrast effects observed are necessary. In such cases it would